Am J Cancer Res 2021;11(8):3877-3892
www.ajcr.us /ISSN:2156-6976/ajcr0134817

Original Article

bFGF-mediated phosphorylation of δ-catenin increases its protein stability and the ability to induce the nuclear redistribution of β-catenin

Gen Chen[1,2], Ning An[3], Yu Zhu[2], Rui Zhou[4], Myung-Giun Noh[5], Hangun Kim[4], Hyoung Jae Lee[1], Yingjie Shen[1,2], Young-Chang Cho[1], Litai Jin[2], Weitao Cong[2*], Jae-Hyuk Lee[6*], Kwonseop Kim[1*]

[1]College of Pharmacy, Chonnam National University, Gwangju 61186, Korea; [2]School of Pharmaceutical Science, Wenzhou Medical University, Wenzhou 325000, P. R. China; [3]Department of Pharmacy, Ningbo Medical Center Lihuili Hospital, Ningbo 315041, P. R. China; [4]College of Pharmacy, Sunchon National University, Sunchon 57922, Korea; [5]Department of Biomedical Science and Engineering, Gwangju Institute of Science and Technology (GIST), Gwangju 61005, Korea; [6]Chonnam National University Hwasun Hospital & Medical School, Hwasun 58128, Korea. [*]Equal contributors.

Received April 29, 2021; Accepted June 25, 2021; Epub August 15, 2021; Published August 30, 2021

Abstract: Recently, we have shown that δ-catenin strengthened the epidermal growth factor receptor (EGFR)/Erk1/2 signaling pathway through the association between EGFR and δ-catenin. Now, we further analyzed the correlation between basic fibroblast growth factor (bFGF)/fibroblast growth factor receptor 1 (FGFR1) and δ-catenin in prostate cancer and investigated the molecular mechanism underlying the role of bFGF/FGFR1 modulation in CWR22Rv-1 (Rv-1) cells. Here, we demonstrated that bFGF phosphorylated the tyrosine residues of δ-catenin in Rv-1 cells and further proved that the bFGF mediated FGFR1/δ-catenin tyrosine phosphorylation was time dependent. Furthermore, we demonstrated that bFGF stabilized the expression of δ-catenin through weakening its association with GSK3β and enhancing its stability to induce β-catenin into the nuclear by strengthening the processing of E-cadherin. In a word, these results indicated that bFGF/FGFR1 signaling pathway could enhance the tumor progression of prostate cancer via δ-catenin.

Keywords: δ-catenin, bFGF, FGFR1, E-cadherin, GSK3β

Introduction

δ-Catenin, encoded by *CTNND2* gene, is a member of the p120-catenin (hereafter, p120) subfamily of armadillo proteins and was first identified through its interaction with presenilin-1 [1]. Although δ-catenin is abundantly expressed in developing neurons, it was recently found in a series of human malignancies, such as lung [2], colorectum [3], ovarian [4], and prostate cancer [5, 6]. Furthermore, δ-catenin is highly expressed in a variety of prostate cancer cell lines and promotes the tumorigenesis and growth by improving the expression profiles of survivor-related genes and cell cycle [7]. Previously, we shown that δ-catenin also inhibited the degradation of hypoxia-inducible factor 1-alpha (HIF-1α), thereby increasing the transcription of the downstream transcription factor vascular endothelial growth factor (VEGF), which promoting angiogenesis and increasing prostate tumor nutrient supply in a hypoxic environment [8]. However, RNAi screen for suppressors of epithelial cell transformation cells revealed that δ-catenin maybe as a potential suppressor in some way [9]. Therefore, these studies indicate that δ-catenin plays a critical role in human malignancies, and its biological function in tumorigenesis remains to be further elucidated.

E-cadherin, a kind of classical cadherin that penetrates the cell membrane and participates in the intercellular connection and signal exchange, contains a cytoplasmic, a transmembrane and an extracellular domain [10]. Previously shown that the function of E-cadherin in epithelial cells is often closely related

to the process of tissue canceration and cancer progression, because the down-regulation or even deletion of E-cadherin in most epithelial cancer tissues promoted the loss of normal epithelial morphology and strengthened the ability of metastatic and invasiveness. However, the regulation of E-cadherin depends upon transcription [11] and/or post-transcriptional modification (PTM) [12, 13]. Also, there is considerable evidence that the E-cadherin process involves a variety of proteases and affects varietal cellular functions due to the loss or gain of E-cadherin, including proliferation, migration, adhesion and invasion/metastasis [14]. In our previous study, δ-catenin strengthen the fragment of E-cadherin, resulting in an increase in the total protein level and inducing the nuclear redistribution of β-catenin, which increase transcriptional activity of β-catenin/LEF-1 [15]. These results indicate that δ-catenin could strengthen the signal transduction capacity of β-catenin and that δ-catenin has similar signal transduction function to β-catenin.

Basic fibroblast growth factor (bFGF), as a multifunctional growth factor, is regulated by the FGF receptor 1 (FGFR1) [16], which transmit different biological signals for intracellular protein with cell surface heparin sulfate proteoglycan and heparin [17]. A large number of studies have shown that bFGF promoted angiogenesis and cell proliferation, which protecting the damaged repair of cells and tissues. However, bFGF also regulates tumorigenicity and metastasis of various malignant tumors [18, 19], and is associated with the inferior survival of prostate cancer patients [20]. Although, we previously shown that, δ-catenin strengthened the stability of epidermal growth factor receptor (EGFR) and strengthened the EGFR/extracellular signal-related kinase 1/2 (Erk1/2) signaling pathway through the association between δ-catenin and EGFR [21], whether δ-catenin is regulated by bFGF and then promotes the progression and proliferation of prostate cancer remains to be further elucidated.

Thus, we indicated that bFGF phosphorylated tyrosine δ-catenin in Rv-1 and further proved that the bFGF mediated FGFR1/δ-catenin tyrosine phosphorylation was time dependent. Furthermore, we demonstrated that bFGF stabilized the expression of δ-catenin through weakening its association with GSK3β and enhancing its stability to induce the β-catenin into the nuclear by strengthening the processing of E-cadherin.

Materials and methods

Plasmids

The constructs of δ-catenin wild type (WT), ΔN85-325 in pEGFP-C1 have been previously described [22]. The deletion constructs of 1-1070 were generated by PCR amplification and cloned into pEGFP-C1 vector. mCherry-FGFR1 (Contrast number: HYKY-201229006-DPL) was constructed and purchased from OBiO Technology (Shanghai) Corp., Ltd.

Cell culture and transfection

293T (human epithelial kidney) cells were cultured in RPMI1640 supplemented with 10% FBS and 1% penicillin/streptomycin at 37°C with 5% CO_2. CWR22Rv-1 (human prostate cancer cell line, Rv-1) was cultured in RPMI1640 supplemented with 1% penicillin/streptomycin and 10% fetal bovine serum (FBS) in a 37°C, 5% CO_2 cell incubator. Rv/δ (Overexpression of mouse δ-catenin-GFP in Rv-1 [22]) and Rv/C (Overexpression of green fluorescent protein GFP in Rv-1) were established and selected with G418 (200 μg/ml, Sigma-Aldrich) at 37°C with 5% CO_2. All experiments were performed with mycoplasma-free cells. Plasmid DNA, δ-catenin siRNA (sc-43021, Santa Cruz Biotechnology) or FGFR1 siRNA (SC-29316, Santa Cruz Biotechnology) was used to transfected cells with Lipofectamine™ 2000 reagent (Invitrogen) for 24 h. Before performing a series of experimental procedures, the RPMI1640 medium with 10% FBS was removed and replaced with serum-free medium for 2 h, then cells were treated in the presence or absence of bFGF (20 ng/mL, 233-FB, Novus Biologicals) for 5 min, as previously described [23].

Immunoblotting and immunoprecipitation

Immunoblotting and immunoprecipitation were performed as previously described [24]. Western blot analysis: proteins were separated by SDS-PAGE and transferred to polyvinylidene difluoride membrane which was incubated with an appropriate primary antibody overnight. Blots were visualized using enhanced chemiluminescence (ECL from GE Healthcare, Braunschweig, Germany). Bands were quantified using Quantity One Software (Biorad).

Immunoprecipitation: Rv-1, Rv/C and Rv/δ were lysed with buffer (137 mM NaCl, 20 mM Tris-HCl, 1% NP-40, 2 mM EDTA, 50 mM NaF, 0.1 μM aprotinin). After incubating with primary antibodies and agarose beads overnight at 4°C and washing with lysate buffer 3 times, immunoprecipitates were eluted with 2× sample buffer (4% SDS, 0.1 M Tris-HCl, 20% glycerol, 0.2% bromophenol blue, 0.2 M DTT, pH 6.8), separated and detected by immunoblotting. Cell lysates were also subjected to immunoprecipitation with either mouse IgG1 isotype control (Cell Signaling Technology, 5415) or rabbit IgG isotype control (Cell Signaling Technology, 3900) according to the immunoglobulin type of primary antibody.

Primary antibodies included: anti-lamin B (SC-6216, Santa Cruz Biotechnology), anti-E-cadherin (#610182, BD Bioscience), anti-p-GSK3α/β$^{Ser21/9}$ (#9331, Cell Signaling Technology), anti-δ-catenin (#611537, BD Bioscience), anti-GSK3α/β (#5676, Cell Signaling Technology), anti-β-catenin (#C2206, Millipore Sigma-Aldrich), anti-FGFR1 (#9740, Cell Signaling), anti-GFP (#SC9996, Santa Cruz Biotechnology), anti-py20 (SC-508, Santa Cruz Biotechnology), anti-Flag (#8146, Cell Signaling Technology), anti-β-actin (#A5441, Millipore Sigma-Aldrich) and anti-HA-Tag (#1666851, Boehringer Mannheim).

Isolation of nuclear and cytosolic extracts

The isolation of nuclear, cytosolic and membrane extracts was performed in prostate cancer cells as previously described [25].

Wound healing scratch assay

Cell migration was determined using the wound healing scratch assay. Cells were cultured on 12-well plates and grown overnight until they formed forming a confluent monolayer and a scratch was made using a 10 μL pipette tip. Images of the wounded cell monolayers were taken using a microscope (EVOS, Thermo Fisher Scientific) at 0 and 36 h after wounding and processed using ImageJ software. All experiments were performed with mitomycin-C treatment (10 μM, S8146, Selleck Chemicals) [26] to inhibit cell proliferation.

Transwell assay

Transwell assay was performed to evaluate cell invasion and migration abilities. Briefly, prostate cancer cells were placed in the upper chamber containing serum-free RPMI1640 with or without 20 ng/mL bFGF and the lower chamber was added 10 μg/ml fibronectin as a chemotactic agent. For invasion assays, the upper chamber was coated with 1% gelatin. The cells adhering to the underside of the membrane were stained with 0.2% crystal violet and observed under a light microscope and photographed. Ten fields were selected to count the number of cells to reflect cell mobility [27].

Luciferase assay

The Rv-1 cells transfected with T-cell factor/lymphoid-enhancing factor (TCF/LEF)-Luc reporter plasmid (Qiagen) using Lipofectamine™ 2000 reagent and verified the level of activation of the β-catenin signaling pathway. After that, the cells were seeded into six-well plates and co-treated with or without bFGF for 24 h. According to the instructions provided by the reagent vendor, we used the luciferase assay kit (Promega-Biosciences) to detect the collected cells and analyze TCF/LEF activity (BioTeK Synergy HT microplate reader).

RNA isolation and quantitative real-time PCR (qRT-PCR)

Total RNA was extracted from the CWR22Rv-1 using TRIzol Reagent (Invitrogen, 15596018) according to the manufacturer's instructions. Next, total RNA (2 μg) was reverse transcribed into cDNA using the GoScript Reverse Transcription Kit (Promega, A5001). Quantitative RT-PCR analysis was performed using Power-Up SYBR Green Master Mix (Thermo Fisher Scientific, A25918). The data were analyzed and normalized with β-actin. The primer sequences are listed as follows:

c-Jun	GGTCATGCTCTGTTTCAGGA	GACTGCAAAGATGGAAACGA
cyclin D1	CCTCCTTCTGCACACATTTGAA	GCTGCGAAGTGGAAACCATC
cyclin E1	AAGGAGCGGGACACCATGA	ACGGTCACGTTTGCCTTCC
c-Myc	CTCTCAACGACAGCAGCCCG	CCAGTCTCAGACCTAGTGGA
β-actin	GTTGTCGACGACGAGCG	GCACAGAGCCTCGCCTT

Comparative analysis of transcriptomic data from public resources

We downloaded the mRNA expression profiles and clinical information on 493 prostate adenocarcinomas of TCGA samples available on cBioportal for Cancer Genomics (https://www.

cbioportal.org) [28-30]. And we obtained the PSA information of those patients from firebrowse (http://firebrowse.org/?cohort=prad). For gene expression values, log2 transformed values were used. For FGF signaling pathway score analysis, gene set variation analysis (GSVA) was performed using the PID_FGF_PATHWAY with the GSVA package (version 1.36.3) in the R-4.0.2 program [31, 32]. In the GSVA package, the "ssGSEA" method was selected and analyzed with a minimum size of 10 and a maximum size of 500. Statistical analysis was performed using the R-4.0.2 program for Mac OS. Linear correlations were determined using the Pearson correlation with the function ggscatter from the R-package ggpubr (version 0.4.0). Kruskal-Wallis test was used to compare differences of *CTNND2* expression between Gleason score groups. *P*-value of < 0.05 was considered as statistical significance.

Results

bFGF phosphorylates δ-catenin in an FGFR1-dependent but cytoplasmic tyrosine kinase-independent manner

The final outcomes of increased bFGF signaling includes enhanced metastasis and proliferation, resistance to chemotherapy, radiation and cell death, increased invasiveness, motility and angiogenesis, all of which contribute to prostate tumor progression and clinical aggressiveness [33]. To verify the optimal time and action intensity of bFGF activating protein phosphorylation in the Rv-1 cells line, time- and dose-dependent experiments for bFGF were performed. The level of p-Erk1/2 was significantly increased by bFGF (20 ng/ml, 5 min; Supplementary Figure 1A, 1B). Additionally, the ratio of p-Erk1/2 in Rv/C was similar as Rv/δ cells after 5 min bFGF treatment (Supplementary Figure 1C). However, the expression of py20 in Rv/δ cells was significantly increased than that in Rv/C cells with or without bFGF treatment (Supplementary Figure 1D). These result suggested that δ-catenin enhanced some bFGF/tyrosine signaling pathway. We next determined whether bFGF induced the δ-catenin phosphorylation in both cells, and then performed an immunoprecipitation assay (Supplementary Figure 2A). The tyrosine phosphorylation level of δ-catenin in Rv/C cells was significantly lower than that in Rv/δ cells (**Figure 1A**, **1B**; Supplementary Figure 2B). Furthermore, the immunoprecipitation assay revealed that bFGF treatment increased the association between δ-catenin and FGFR1 in Rv/δ cells (**Figure 1A**, **1D**; Supplementary Figure 2B).

Previous studies reported that bFGF could activate some tyrosine kinases [34]. To further investigate whether bFGF phosphorylates δ-catenin in an FGFR1-dependent but cytoplasmic tyrosine kinase-independent, Rv/δ cells were pretreated with FAK (PF431396, 500 nM), Src (SU665, 100 nM) and JAK (CP690550, 500 nM) kinase inhibitors. We found that these kinase inhibitors did not affect the efficacy of bFGF, which only acts on the respective kinases and no regulation of feedback (**Figure 1C**). Furthermore, the phosphorylation level of δ-catenin was mildly decreased after inhibitor treatments (**Figure 1C**; Supplementary Figure 2C, 2D), suggesting that the bFGF mediated δ-catenin tyrosine phosphorylation was mainly FGFR1 dependent. Next, to determine whether bFGF/FGFR1-induced phosphorylation of δ-catenin required FGFR1, we used the FGFR1-deficient RV-1 cells and found that no tyrosine phosphorylated δ-catenin was observed. However, when we overexpressed FGFR1 in FGFR1-deficient RV-1 cells, tyrosine phosphorylation of δ-catenin was detectable, suggesting that bFGF-induced phosphorylation of δ-catenin was indeed FGFR1-dependent (**Figure 1E**, **1F**). In conclusion, these results indicated that bFGF promoted the association between FGFR1 and δ-catenin, which induced the phosphorylation of δ-catenin.

bFGF mediated δ-catenin tyrosine phosphorylation by FGFR1 was time-dependent

Interestingly, we found that the change in the bFGF-induced phosphorylation of δ-catenin (average 2.40-fold) was significantly greater than the change in the interaction between FGFR1 and δ-catenin (1.43-fold) in the presence or absence of bFGF (**Figure 1A**, **1B** and **1D**). Additionally, the immunoprecipitation assay revealed that bFGF treatment mildly decreased the association between FGFR1 and δ-catenin in Rv/C cells (**Figure 1A**). Therefore, we investigated whether the mechanism underlying the interaction between FGFR1 and

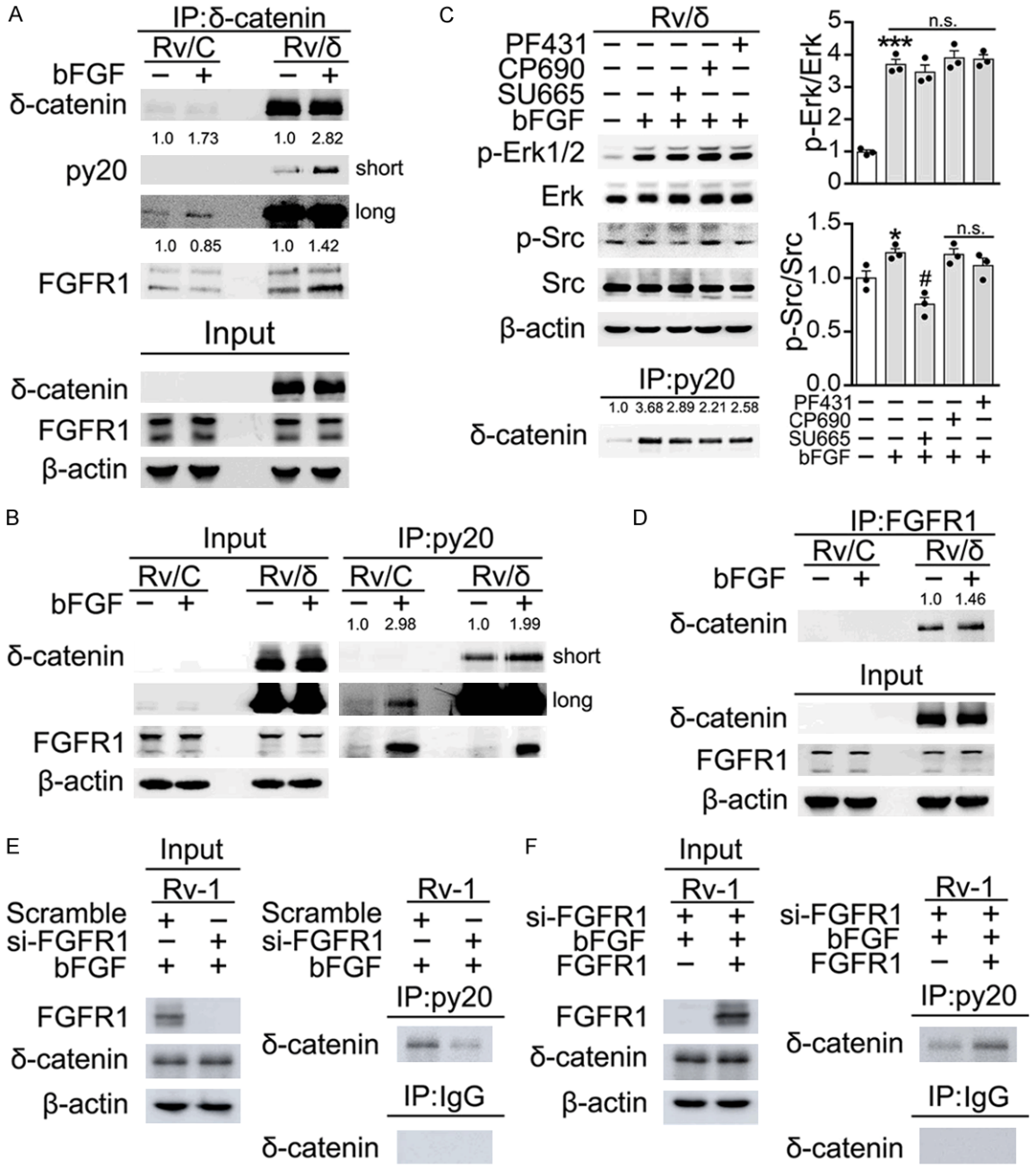

Figure 1. δ-Catenin is phosphorylated by bFGF in an FGFR1 dependent but cytoplasmic tyrosine kinase independent manner. Rv/C and Rv/δ cells were derived from Rv-1 cells, overexpressing either GFP or mouse GFP-δ-catenin, respectively. They were cultured in serum-free medium in the presence or absence of bFGF (20 ng/ml) for 5 min. A. The cell lysates were subjected to immunoprecipitation with anti-δ-catenin antibody followed by immunoblotting with anti-py20 and anti-FGFR1 antibodies. The tyrosine-phosphorylation of δ-catenin was increased in both Rv/δ and Rv/C cells by treatment with bFGF. B. Reverse immunoprecipitation was performed with anti-py20 antibody followed by anti-δ-catenin and anti-FGFR1 antibodies. C. Rv/δ cells were respectively pretreated with Src (SU665, 100 nM), FAK (PF431396, 500 nM), and JAK (CP690550, 500 nM) kinase inhibitors for 2 h in serum-free medium before harvesting. The cell lysates were used to perform immunoblotting to check the protein expression of p-Erk, Erk, p-Src, Src, and β-actin and were also subjected to immunoprecipitation with anti-py20 antibody followed by immunoblotting with the anti-δ-catenin antibody. The relative protein ratios from at least three independent experiments are shown as a bar graph in the right panel. The values are presented as the mean ± SEM. $^{*}P < 0.05$ vs. control; $^{***}P < 0.001$ vs. control; $^{\#}P < 0.05$ vs. bFGF; n.s. no significant difference. D. Reverse immunoprecipitation was performed with the anti-FGFR1 antibody followed by the anti-δ-catenin antibody. E. FGFR1 siRNA was used to transfected Rv-1 cells with LipofectamineTM 2000 reagent (Invitrogen) for 24 h and cells were treated in the pres-

ence or absence of bFGF (20 ng/ml) for 5 min. The cell lysates were subjected to immunoprecipitation with anti-py20 antibody followed by immunoblotting with δ-catenin antibodies. F. FGFR1 knockout Rv-1 cells (transfected with FGFR1 siRNA) and then transfected with FGFR1 plasmid. Transfected cells were treated with bFGF (20 ng/ml 5 min) and harvested to perform immunoprecipitation with anti-py20 antibody followed by δ-catenin antibody.

δ-catenin was time-dependent, i.e., the phosphorylated δ-catenin would dissociate from FGFR1, and new δ-catenin would bind to FGFR1 later. To verify this hypothesis, Rv/δ cells were cultured in serum-free medium in the presence or absence of bFGF for 5, 10, 20, and 30 min. As shown in **Figure 2A**, the expression of p-Erk1/2 decreased rapidly during the 5- to 30-minute interval. However, the phosphorylated δ-catenin (IP: py20; WB: δ-catenin) decreased slowly (**Figure 2B**). Furthermore, the association between FGFR1 and δ-catenin was always present even without bFGF, and then δ-catenin dissociated from FGFR1 when bFGF treatment after 10 min (**Figure 2C**). Next, we examined bFGF/FGFR1 mainly phosphorylates which fragment of δ-catenin. Rv-1 cells were transfected with the constructs of GFP-δ-catenin WT (FL) and its different deletions [C-terminus (1-1070) or N-terminus (ΔN85-325)] in the presence or absence of bFGF. We found that the downstream bFGF/FGFR1 signaling pathway did not change compared with different groups after bFGF treatment (Supplementary Figure 3A). However, δ-catenin C-terminal deletion significantly weakened bFGF-mediated tyrosine phosphorylation of δ-catenin, while δ-catenin N-terminal deletion had no negative effect on it (**Figure 2D**). To further confirm above results, transfection of mCherry-FGFR1 and GFP-δ-catenin WT or its different deletions was performed in 293 cells (Supplementary Figure 3B). Consistently, bFGF/FGFR1 signaling pathway did not change compared with different groups after bFGF treatment (Supplementary Figure 3C). Additionally, we found that δ-catenin N-terminal deletion, could be much more phosphorylated compared with δ-catenin C-terminal deletion (**Figure 2E**). These results indicated that the bFGF-mediated tyrosine phosphorylation of δ-catenin on its C-terminus was increased through a dynamic balance in the association between FGFR1 and δ-catenin over time.

bFGF stabilizes δ-catenin via interfering the association between GSK3β and δ-catenin

To explore the long-term influence of bFGF on δ-catenin, Rv/C cells were co-cultured with bFGF for 12, 24, 36, and 48 h. Treatment with bFGF for 12-36 h increased δ-catenin protein expression, especially at 36 h, but the expression was subsequently decreased slightly at 48 h compared with that at 36 h (**Figure 3A**). However, bFGF treatment did not affect δ-catenin mRNA levels in the Rv-1 cells (Supplementary Figure 4A). In Rv-1 cells exposed to bFGF and MG132, the protein level of δ-catenin was not significantly different compared with the bFGF group (Supplementary Figure 4B). To investigate whether bFGF increased the δ-catenin by inhibiting degradation, we detected the protein level of δ-catenin after cyclohexylimide (CHX) treatment at different times in Rv/δ cells. Obviously, the half-life of δ-catenin was around 11 h when treated with bFGF, but only around 6 h without bFGF treatment (**Figure 3B**). These findings indicated that bFGF increased δ-catenin stability.

As we studied before that GSK3β negatively regulated its stability through phosphorylated δ-catenin and ubiquitination/proteosome-mediated proteolysis [35]. Therefore, to explore whether the molecular mechanism for bFGF to maintain stability of δ-catenin was contribute to bFGF interferes with the association between GSK3β and δ-catenin. Concordant with our previous observations [35], the protein level of δ-catenin in co-transfected HA-GSK3β was significantly lower than that in controls in the presence or absence of bFGF (**Figure 3C**). To further confirm our conjecture, we used δ-catenin and HA antibodies for performing immunoprecipitation experiments in Rv/δ cells. Additionally, the HA-GSK3β immune complexes were analyzed using δ-catenin antibody or reverse immunoprecipitation (bottom panel), as shown in **Figure 3D**. These results shown that bFGF reduced the association between GSK3β and δ-catenin. Meanwhile, δ-catenin had a lower affinity for HA-ubiquitin modification after bFGF treatment, indicating that bFGF could protect δ-catenin from ubiquitination/proteasome mediated proteolysis (**Figure 3E**). Therefore, these results indicated that bFGF reduced the interaction between GSK3β and δ-catenin, thereby protecting δ-

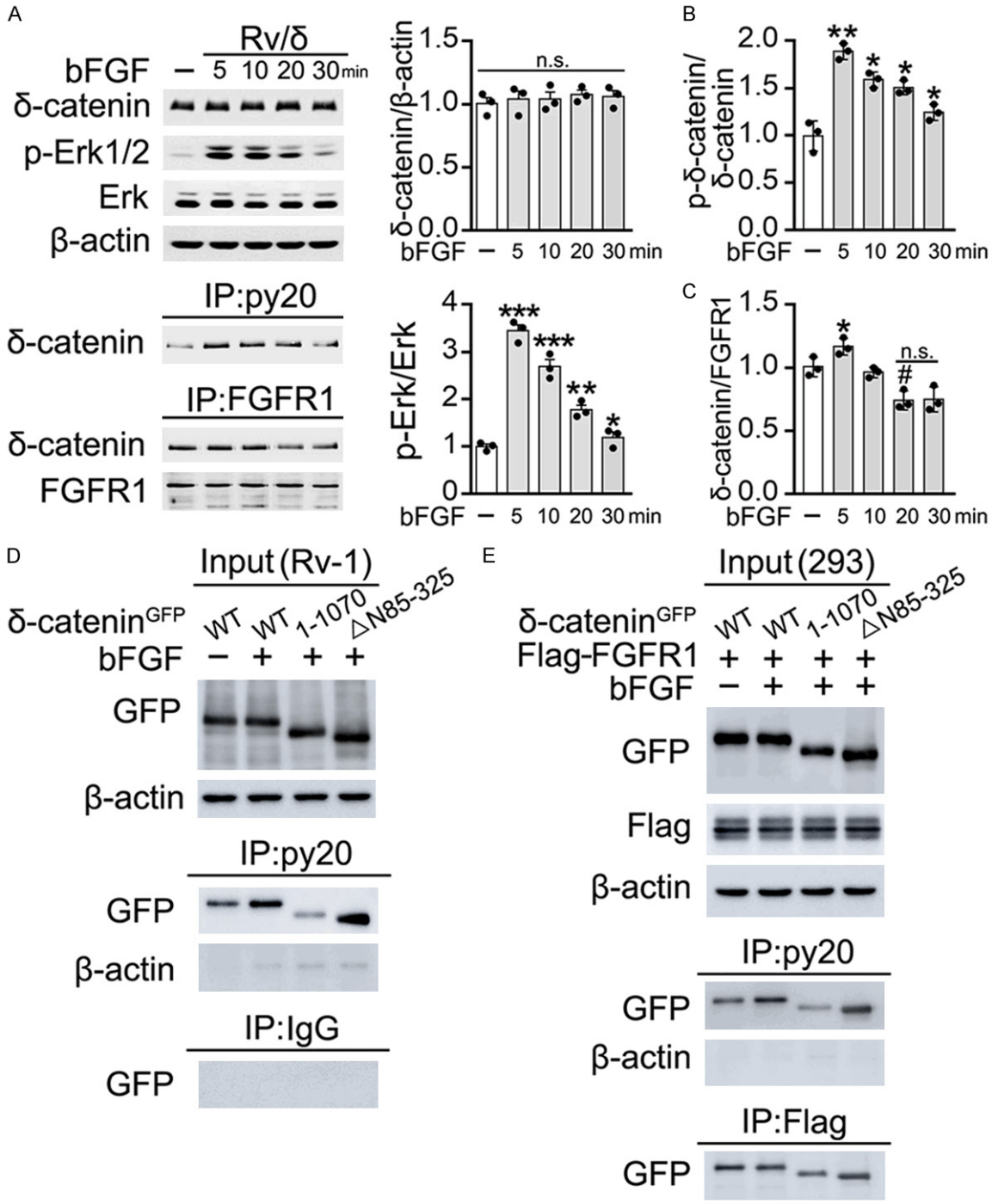

Figure 2. bFGF-mediated tyrosine phosphorylation of δ-catenin by FGFR1 is time dependent. A. Rv/δ cells were cultured in medium in the presence or absence of bFGF (20 ng/ml) for 5, 10, 20, and 30 min. The cells were harvested and the cell lysates were subjected to immunoblotting with specific antibodies to analyze the protein expression. The relative protein ratios from at least three independent experiments are shown as a bar graph in the right panel. All values are presented as the mean ± SEM. $^{*}P < 0.05$ vs. control; $^{**}P < 0.01$ vs. control; $^{***}P < 0.001$ vs. control; n.s. no significant difference. After analyzing the protein expression in the cell lysates, immunoprecipitation experiments were performed with either py20 antibody or FGFR1 antibody followed by immunoblotting with antibody as indicated. B. Quantitative analysis of p-δ-catenin (IP: py20; WB: δ-catenin), the values displayed are the mean ± SEM of three independent experiments in the right panel. $^{*}P < 0.05$ vs. control; $^{**}P < 0.01$ vs. control. C. Quantitative analysis of interaction between FGFR1 and δ-catenin (IP: FGFR1; WB: δ-catenin), the values displayed are the mean ± SEM of three independent experiments in the right panel. $^{*}P < 0.05$ vs. control; $^{\#}P < 0.05$ vs. 5 min bFGF treat-

ment; n.s. no significant difference. D. Tyr-phosphorylation of δ-catenin in Rv-1 cells. Rv-1 cells were transfected with the constructs of GFP-δ-catenin WT and its different deletions (N terminal deletion: 85-325 was deleted; C terminal deletion 1-1070:1071-1247 was deleted) in the presence or absence of bFGF (20 ng/ml 5 min). After harvesting cells, the cell lysates were subjected to immunoprecipitation with relative antibodys and followed by other antibodies. E. Tyr-phosphorylation of δ-catenin in 293 cells. 293 cells were transfected with the constructs of GFP-δ-catenin WT and its different deletions in the presence or absence of bFGF (20 ng/ml 5 min). After harvesting cells, the cell lysates were subjected to immunoprecipitation with relative antibodys and followed by other antibodies.

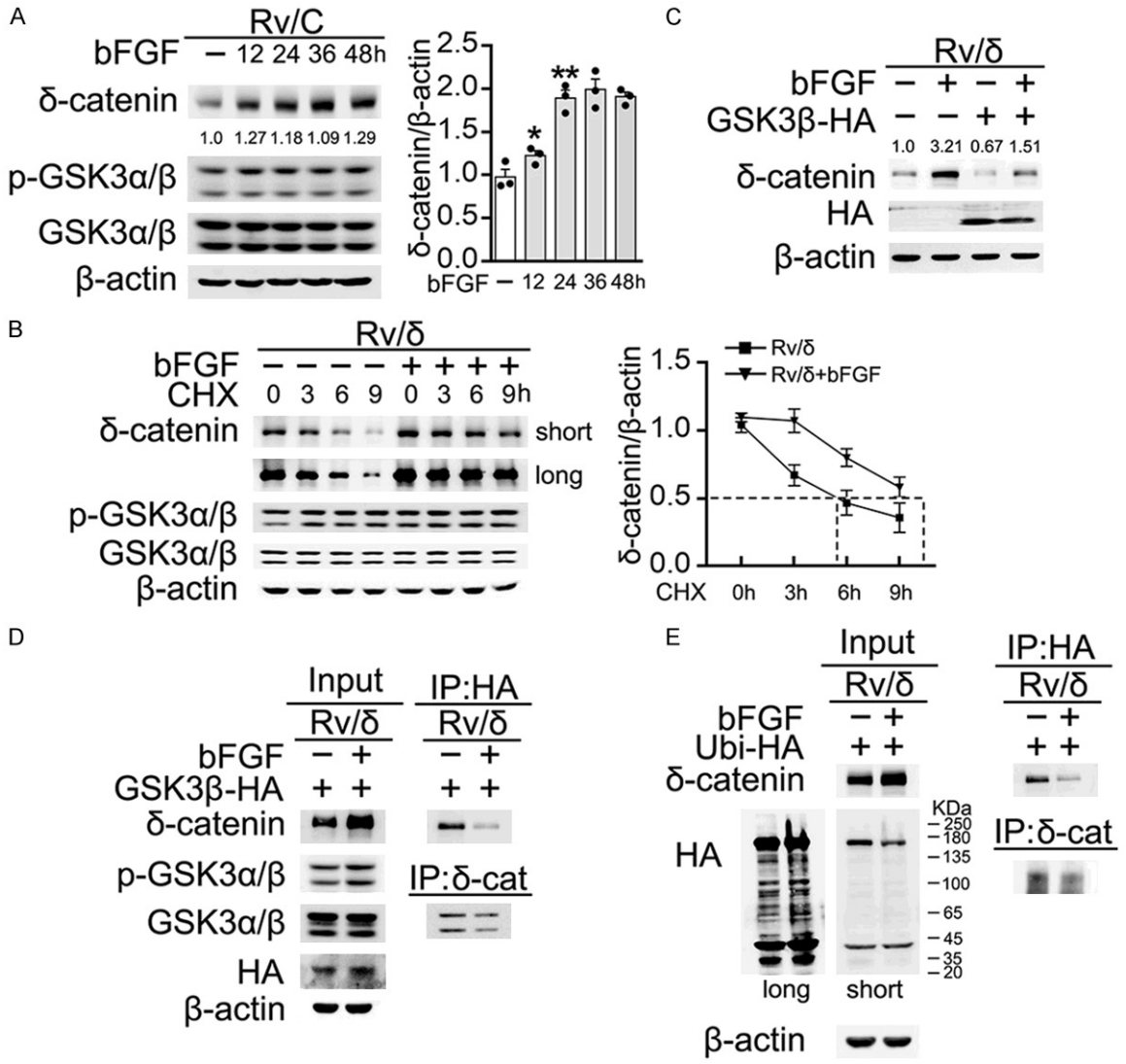

Figure 3. bFGF can stabilize δ-catenin through by interrupting the interaction between δ-catenin and GSK3β. A. Rv/C cells were cultured in medium in the presence or absence of bFGF (20 ng/ml) for 12, 24, 36, and 48 hours. The cells were harvested, and the cell lysates were subjected to immunoblotting with specific antibodies to analyze the protein expression. The relative protein ratios from at least three independent experiments are shown as a bar graph in the right panel. The values are presented as the mean ± SEM. $^{*}P < 0.05$ vs. control; $^{**}P < 0.01$ vs. control. B. Rv/δ cells were treated in the presence or absence of bFGF (20 ng/ml) or cycloheximide (50 μM) for different times as indicated. The cell lysates were collected and subjected to immunoblotting. Right panel: Relative protein levels of δ-catenin. The protein density of the immunoblots was measured by Multi-Gauge, and the protein level of δ-catenin was normalized to the protein level of β-actin. C. Rv/δ cells were transfected with GSK3β-HA and then treated with or without bFGF (20 ng/ml) for 12 h. The cell lysates from the transfected cells were subjected to immunoblotting. D. Rv/δ cells were transfected with GSK3β-HA and then treated with or without bFGF (20 ng/ml) for 12 h. The cell lysates were subjected to immunoblotting with the following antibodies: δ-catenin, GSK3α/β, p-GSK3α/β, HA, and β-actin antibody. After analyzing the protein expression in the cell lysates, immunoprecipitation experiments were performed with either HA antibody or δ-catenin antibody followed by immunoblotting with antibody as indicated. E.

Rv/δ cells were transfected with Ubi-HA and treated with or without bFGF (20 ng/ml) for 12 h. The cell lysates were subjected to immunoblotting with the following antibodies: δ-catenin, HA, and β-actin antibody. After analyzing the protein expression in the cell lysates, immunoprecipitation experiments were performed with either HA antibody or δ-catenin antibody followed by immunoblotting with antibody as indicated.

catenin from the effects of GSK3β-mediated phosphorylation ubiquitination.

bFGF increases δ-catenin ability to induce the β-catenin into the nuclear by strengthening the processing of E-cadherin

Recently, we indicated that δ-catenin could strengthen the processing of E-cadherin, thereby inducing the β-catenin into the nuclear [25]. We found that the action of bFGF altered the fragment of E-cadherin to varying degrees in both cell lines (**Figure 4A**). However, the amount of fragment with a size of about 140 KD (maybe the phosphorylation of E-cadherin) was attenuated in the Rv/C cells than in the Rv/δ cells after bFGF treatment. Additionally, the amount of membrane fragment with a size of about 100 KD decreased, whereas the membrane fragment with a size of about 85 KD increased in the Rv/δ cells only. Interestingly, the amount of fragment with a size of about 50 KD localized to the membrane was significantly greater and the nuclear localization was lower in the Rv/δ cells compared with the Rv/C cells. These results suggested that both bFGF and δ-catenin could regulate the processing of E-cadherin by different mechanisms. Consistently, δ-catenin was stabilized by bFGF detectably, mainly in the fraction of membrane and somewhat in the fraction of nuclear but not in the fraction of cytoplasmic (Supplementary Figure 5A).

We next tested whether bFGF mediated β-catenin into the nuclear via δ-catenin by immunoprecipitation (Supplementary Figure 5B). Consistently, the binding effect between E-cadherin and β-catenin was attenuated after bFGF co-treatment. However, the decrease of affinity in Rv/δ cells was significantly increased than that of Rv/C cells. In parallel, bFGF treatment attenuated the binding effect between E-cadherin and δ-catenin in both cell lines. Furthermore, we found that the indirectly binding effect between δ-catenin and β-catenin was attenuated by bFGF treatment of Rv/δ cells due to E-cadherin processing (**Figure 4B**; Supplementary Figure 5C).

Additionally, we examined whether the dissociated β-catenin in the cytoplasm entered the nucleus or underwent degradation. We found that bFGF increased the nuclear localization of β-catenin in both cell lines, while the distribution of β-catenin in Rv/δ cells was significantly increased than that in Rv/C cells (**Figure 4C**). Furthermore, to determine whether the effect of bFGF was partly δ-catenin-mediated, the si-δ-catenin was transfected into Rv-1. We found that bFGF and si-δ-catenin combined treatment decreased the expression of a battery of proliferation-associated genes in Rv-1 cells (**Figure 4D**). Additionally, we found that the transcription of β-catenin/LEF-1 was greatly increased in Rv-1 cells after bFGF treatment. However, the bFGF-mediated transcription of β-catenin was partly blocked after transfecting with si-δ-catenin (**Figure 4E**). Additionally, the migration and invasion abilities were also significantly increased by bFGF treatment in both cells compared with control prostate cancer cells. Importantly, the increase in motility in Rv/δ cells was greater than that in Rv/C cells when treated with bFGF (**Figure 5A**, **5B**). However, transfected with si-δ-catenin into Rv-1 cells significantly impaired the migration and invasion abilities exposed to bFGF treatment (Supplementary Figure 6A, 6B). In addition, wound healing scratch assay showed that the migration was decreased in the cells with si-δ-catenin compared with that cells with si-Scramble even have bFGF treatment (Supplementary Figure 6C). In summary, bFGF increased the δ-catenin ability to induce β-catenin into the nuclear by strengthening the processing of E-cadherin and thereby enhancing the tumor progression of prostate cancer.

Comparative analysis of transcriptomic data from public resources

Recently, Lu Q et al. showed that the expression of δ-catenin in patients with prostate cancer is more highly than in healthy individuals and its expression was correlated with increasing Gleason scores [5]. To further study the role of FGF signaling pathway in prostate cancer, we performed the comparative analysis of

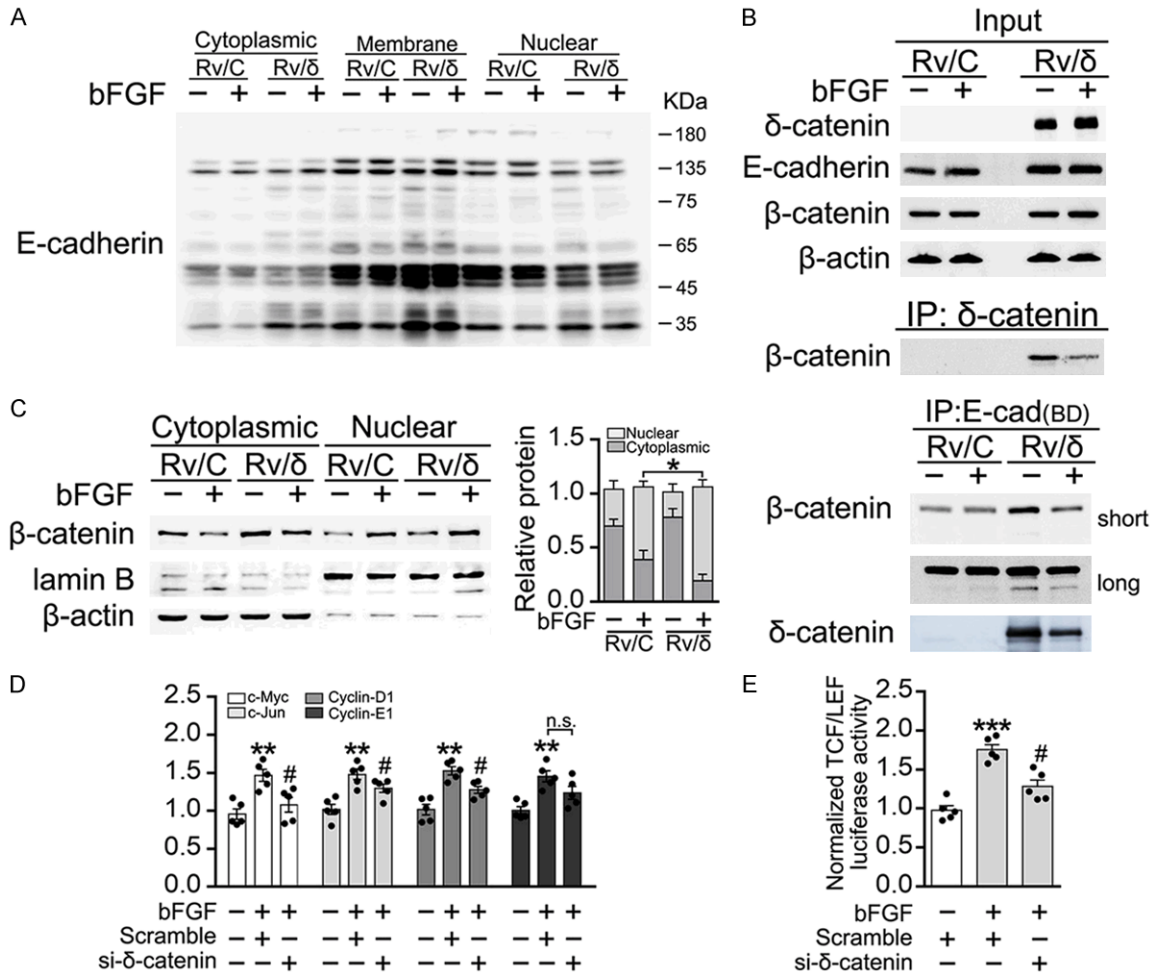

Figure 4. bFGF increases δ-catenin ability to enhance the nuclear distribution of β-catenin by disturbing the integrity of E-cadherin. A. Both Rv/δ and Rv/C cells were treated with bFGF for 12 h and subjected to the fractionation experiment. The membrane fractions were subjected to immunoblotting with anti-E-cadherin. B. Both Rv/δ and Rv/C cells were treated with bFGF for 12 h. The cells were harvested, and the lysates were used to perform immunoblotting with the following antibodies: δ-catenin, β-actin, E-cadherin, and β-catenin antibody. After analyzing protein expression, the cell lysates were subjected to immunoprecipitation with δ-catenin or E-cadherin antibody followed by immunoblotting with antibody as indicated. C. Both Rv/δ and Rv/C cells were treated with bFGF for 12 h and subjected to the fractionation experiment. The protein expression of β-catenin in each lysate was analyzed by immunoblotting. The relative β-catenin ratios from at least three independent experiments are shown as a bar graph in the right panel. The values are presented as the mean ± SEM. $^{*}P < 0.05$. D. The mRNA expression of *c-Myc*, *c-Jun*, *cyclin-D1*, and *cyclin-E1* genes in Rv-1 cells. The values displayed are the mean ± SEM of five independent experiments. The two-tailed Student's t-test was used, n.s. = not significant, $^{**}P < 0.05$ vs. control; $^{\#}P < 0.05$ vs. bFGF. E. TEF/LEF-luciferase reporter activity in Rv-1 cells. The values displayed are the mean ± SEM of five independent experiments. $^{***}P < 0.001$ vs. control; $^{\#}P < 0.05$ vs. bFGF.

transcriptomic data in 493 prostate cancer patients dataset of the cancer genome atlas (TCGA) published in the Cbioportal database and Firebrowse. By linear correlation analysis, gene expression level of *CTNND2* was significantly correlated with prostate specific antigen (PSA) level ($R = 0.095$ and $P = 0.048$) (**Figure 6A**). As the Gleason score increased, the expression value of the *CTNND2* gene also showed a tendency to increase (**Figure 6B**). Additionally, the linear correlation analysis revealed that FGF signaling pathway score showed a significantly positive correlation with the gene expression of *CCND1* (Cyclin D1) *and JUN* ($P = 0.023$ and $P < 0.001$, respectively), however, significantly negative correlation with the gene expression of *CTNND2* ($P = 0.038$) (**Figure 6C**). These results demonstrated that

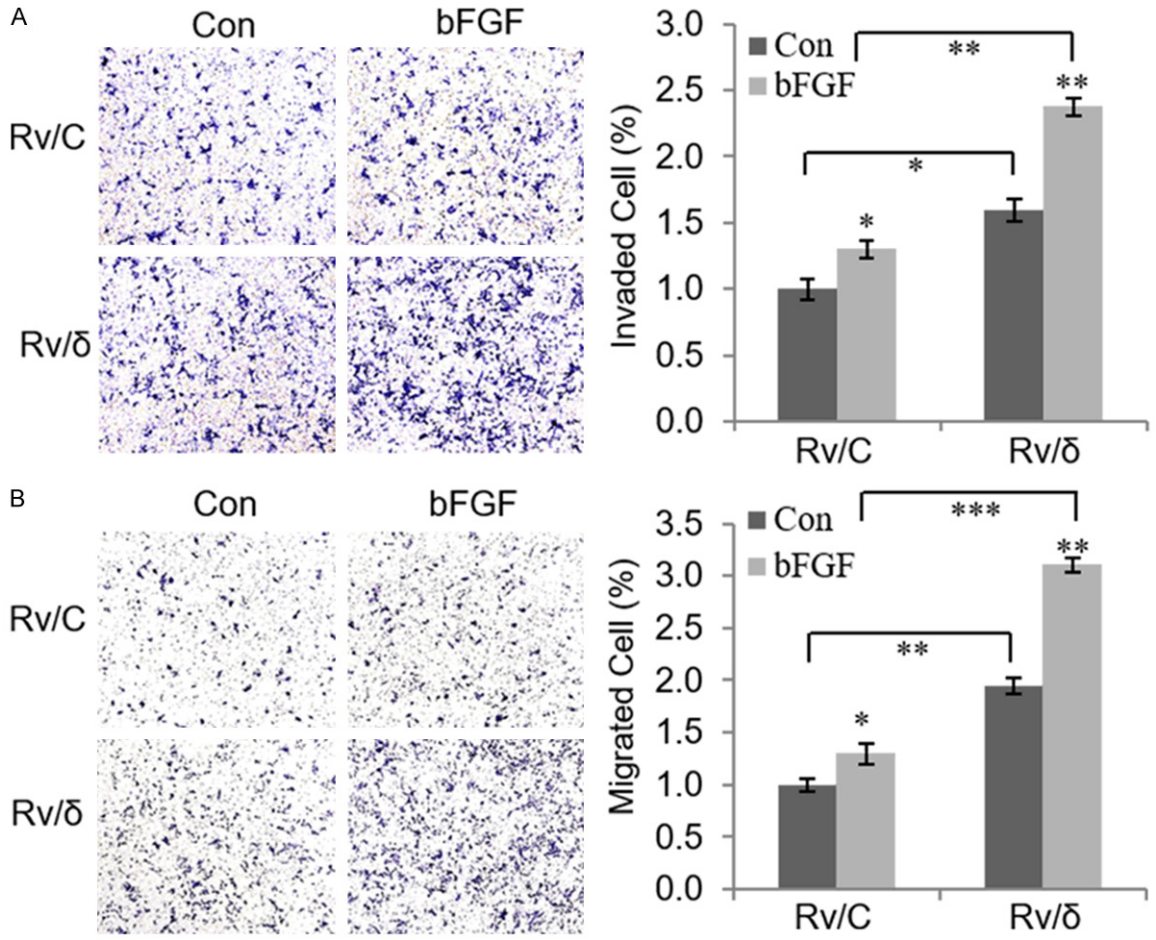

Figure 5. bFGF increase the migration and invasion abilities in prostate cancer cells. (A, B) Invasion and migration assays were performed in the presence or absence of bFGF. Transwell chambers coated with (A) or without (B) gelatin, respectively. Quantitative analysis of cell viability, colony area, and migrated and invaded cell numbers from at least three independent experiments are shown as a bar graph in each right panel. The values are presented as the mean ± SEM. $^{*}P < 0.05$; $^{**}P < 0.01$; $^{***}P < 0.001$.

the molecular mechanisms of bFGF-mediated phosphorylation of δ-catenin and its increased protein stability, rather than its transcriptional control of *CTNND2*, provided a potential therapeutic target for inhibiting prostate cancer.

Discussion

Tumor progression is the result of an imbalance between cellular functions including apoptosis, division, cell growth, and adhesion. Among the many oncogenes and tumor suppressors, cellular connection-related proteins, such as adenomatous polyposis coli (APC) and β-catenin, contribute to tumor progression by interfering with E-cadherin-based junctions and cell proliferation, as well as reducing apoptosis and altering the karyotype [36, 37].

δ-Catenin, or NPRAP (neural plakophilin-related armadillo protein)/neurojungin, is an adhesion connection-related protein originally identified a neural-specific protein [1, 3, 38, 39]. Moreover, δ-catenin belongs to the p120ctn subgroup of the armadillo/β-catenin superfamily [38, 40]. Under normal conditions, p120ctn and β-catenin are widely expressed in bodies, while the δ-catenin in healthy individuals is mainly confined to the brains. Interestingly, δ-catenin is increasingly reported to be highly expressed in varietal cancers in peripheral tissues [2-4, 41]. Recently, Lu Q et al. showed that the expression of δ-catenin in patients with prostate cancer is more highly than in healthy individuals and its expression was correlated with increasing Gleason scores [5].

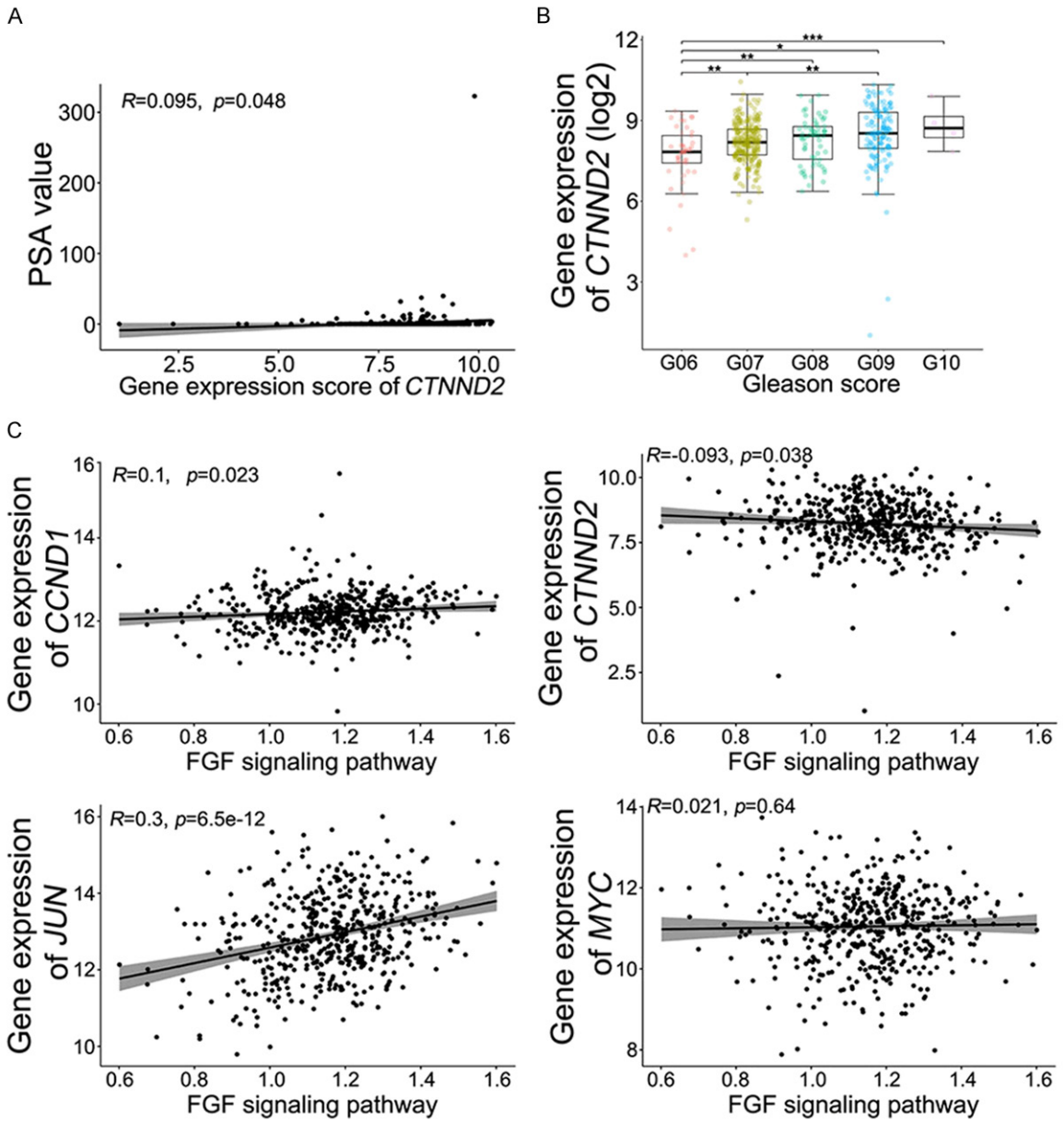

Figure 6. Comparative analysis of transcriptomic data from public resources. A. Linear correlation analysis of gene expression of *CTNND2* and PSA level (ng/mL). The Pearson's correlation was used. B. Box plots showing that the expression level of *CTNND2* showed a tendency to increase as the Gleason score increased. The Kruskal-Wallis test and Fisher's Least Significant Difference test were used. C. Linear correlation analysis of FGF signaling pathway score and gene expression level of CCND1 (left, upper), CTNND2 (right, upper), JUN (left, lower) and MYC (right, lower). $^{*}P < 0.05$; $^{**}P < 0.01$; $^{***}P < 0.001$.

Basic fibroblast growth factor is one of the primary angiogenic peptides associated with tumor vascularization [19, 42-45]. The elevated expression of bFGF has been demonstrated in many tumor cell lines, including those derived from prostate cancer [46-48]. In addition, the aberrant bFGF signals could directly drive the proliferation and survival of prostate cancer cells, and then support tumor angiogenesis and promoting tumor development in various prostate cancer models [49]. Furthermore, elevated levels of bFGF was also observed in urine and serum in some prostate cancer patients [50]. Mechanistically, bFGF activated multiple mitogen-activated protein kinases (MAPKs) such as p38, c-Jun N-terminal kinase

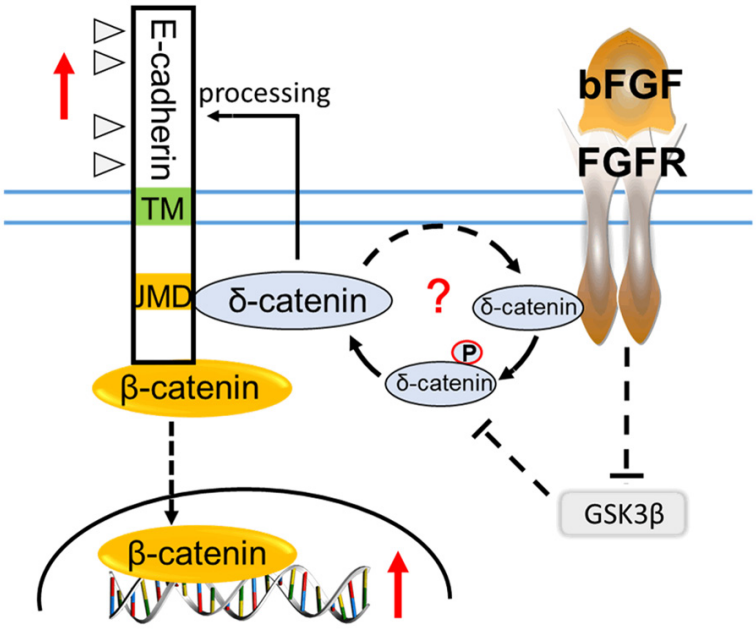

Figure 7. Schematic illustration of the effects of bFGF via δ-catenin in prostate cancer. bFGF phosphorylates δ-catenin on its tyrosine residues in prostate cancer cells and further prove that bFGF-mediate tyrosine phosphorylation of δ-catenin by FGFR1 is time dependent. In addition, bFGF stabilizes δ-catenin protein expression via decreasing its affinity to GSK3β and enhances its ability of inducing nuclear distribution of β-catenin through interfering the integrity of the E-cadherin complex. Taken together, these results indicate that bFGF/FGFR1 can enhance the motility function of δ-catenin in prostate cancer cells.

(JNK) and Erk [51-53] as well as the phosphatidylinositol 3-kinase (PI3K)/AKT pathway [54]. These pathways are critical for the progression of prostate cancer, including proliferation, differentiation, and survival [55, 56].

In this study, we found that Rv-1 cells express the endogenous δ-catenin and FGFR1, which allow knock-down experiments to verify our findings. However, both LnCap and DU145 cell lines do not express detectable levels of endogenous δ-catenin as we have published before [57]. Therefore, we used Rv-1 cells as a study subject and found that bFGF could (1) phosphorylate the δ-catenin tyrosine residues by FGFR1 in time-dependent manner and (2) increase the stability of δ-catenin, inducing β-catenin in the cytoplasm entered the nucleus by attenuating the binding effect between GSK3β and δ-catenin, and improving the processing of E-cadherin.

The first innovative finding of this study was that bFGF mediated FGFR1/δ-catenin tyrosine phosphorylation was time dependent. We found that the association between FGFR1 and δ-catenin was always present even without bFGF treatment and that the phosphorylation of δ-catenin accumulated through a dynamic balance of the interaction between FGFR1 and δ-catenin mediated by bFGF. In addition, the C-terminus of δ-catenin is necessary for bFGF/FGFR1-mediated phosphorylation. Unfortunately, bFGF was shown to regulate the phosphorylation of δ-catenin, but whether FGFR1 and δ-catenin bind directly or form a complex remains unknown.

Secondly, we found that bFGF could decrease the association between GSK3β and δ-catenin through bFGF/FGFR1-mediated phosphorylation, which contribute to stabilize the expression of δ-catenin in Rv/C cells. Therefore, three possible mechanisms underlie our observation could be that: a) bFGF protected δ-catenin from phosphorylation by GSK3β and its subsequent degradation by proteasome; b) bFGF increased the level of transcription for δ-catenin and c) bFGF had an effect on the regulation of both mechanisms mentioned above. As expected, bFGF decreased the association between δ-catenin and GSK3β, but did not change the level of transcription of δ-catenin. Furthermore, bFGF/FGFR1 signaling pathway enhanced the tumor progression of prostate cancer via δ-catenin, which is a little same as we previously discovered [15]. Next, we found that decreasing association between GSK3β and δ-catenin made δ-catenin more stable and thus increased the half-life of degradation. As we know, both p120ctn and δ-catenin interacted with the proximal membrane domain of E-cadherin with different biological functions. Particularly, overexpression of δ-catenin in primary prostatic adenocarcinomas was usually accompanied by decreased expression of p120ctn and E-cadherin, and it's also contribute to the redistribution of p120ctn and E-cadherin in prostate cancer

cells [5]. Here, we indicated that δ-catenin was stabilized by bFGF detectably, mainly in the fraction of membrane and somewhat in the fraction of nuclear but not in the fraction of cytoplasmic. Moreover, the binding effect between β-catenin and E-cadherin was attenuated by bFGF co-treatment, and then increased the δ-catenin ability to induce β-catenin into the nuclear by strengthening the processing of E-cadherin.

In summary, we associated with both δ-catenin and bFGF/FGFR1, reaffirming it as a potential target for primary prostatic adenocarcinomas treatment. Mechanistically, we indicated that phosphorylated and stabilized δ-catenin by bFGF/FGFR1 could enhance its ability to improve the processing of E-cadherin as well as the nuclear redistribution of β-catenin (**Figure 7**). Taken together, the present study gave a further insight into δ-catenin's biologic function in primary prostatic adenocarcinomas, suggesting the potential predictive value of δ-catenin for prostate cancer.

Acknowledgements

This study was supported by a grant from the National Research Foundation of Korea (NRF), Ministry of Science, Republic of Korea (NRF-2019R1I1A3A01061094).

Disclosure of conflict of interest

None.

Address correspondence to: Weitao Cong, School of Pharmaceutical Science, Wenzhou Medical University, Center North Road, Wenzhou 325000, Zhejiang, P. R. China. Tel: +86-577-86699790; Fax: +86-577-86699790; E-mail: cwt97126@126.com; Jae-Hyuk Lee, College of Medicine, Chonnam National University Hwasun Hospital & Medical School, Hwasun 58128, Korea. Tel: +82-10-9431-9202; Fax: +82-10-9431-9202; E-mail: jhlee@jnu.ac.kr; Kwonseop Kim, College of Pharmacy, Chonnam National University, Bldg.1 Rm211, Gwangju 61186, Korea. Tel: +82-62-530-2949; Fax: +82-62-530-2949; E-mail: koskim@jnu.ac.kr

References

[1] Zhou J, Liyanage U, Medina M, Ho C, Simmons A, Lovett M and Kosik K. Presenilin 1 interaction in the brain with a novel member of the armadillo family. Neuroreport 1997; 8: 2085-90.

[2] Zhang J, Wang Y, Zhang D, Yang Z, Dong X, Jiang G, Zhang P, Dai S, Dong Q, Han Y, Zhang S, Cui Q and Wang E. Delta-catenin promotes malignant phenotype of non-small cell lung cancer by non-competitive binding to E-cadherin with p120ctn in cytoplasm. J Pathol 2010; 222: 76-88.

[3] Zhang H, Dai S, Zhang D, Liu D, Zhang F, Zheng T, Cui M and Dai C. Delta-catenin promotes the proliferation and invasion of colorectal cancer cells by binding to E-cadherin in a competitive manner with p120 catenin. Target Oncol 2014; 9: 53-61.

[4] Fang Y, Li Z, Wang X and Zhang S. Expression and biological role of δ-catenin in human ovarian cancer. J Cancer Res Clin Oncol 2012; 138: 1769-76.

[5] Lu Q, Dobbs L, Gregory C, Lanford G, Revelo M, Shappell S and Chen Y. Increased expression of delta-catenin/neural plakophilin-related armadillo protein is associated with the down-regulation and redistribution of E-cadherin and p120ctn in human prostate cancer. Hum Pathol 2005; 36: 1037-48.

[6] Lu Q, Zhang J, Allison R, Gay H, Yang W, Bhowmick N, Frelix G, Shappell S and Chen Y. Identification of extracellular delta-catenin accumulation for prostate cancer detection. Prostate 2009; 69: 411-8.

[7] Zeng Y, Abdallah A, Lu J, Wang T, Chen Y, Terrian D, Kim K and Lu Q. Delta-catenin promotes prostate cancer cell growth and progression by altering cell cycle and survival gene profiles. Mol Cancer 2009; 8: 19.

[8] He Y, Kim H, Ryu T, Kang Y, Kim J, Kim B, Lee J, Kang K, Lu Q and Kim K. δ-catenin overexpression promotes angiogenic potential of CWR22Rv-1 prostate cancer cells via HIF-1α and VEGF. FEBS Lett 2013; 587: 193-9.

[9] Westbrook T, Martin E, Schlabach M, Leng Y, Liang A, Feng B, Zhao J, Roberts T, Mandel G, Hannon G, Depinho R, Chin L and Elledge S. A genetic screen for candidate tumor suppressors identifies REST. Cell 2005; 121: 837-48.

[10] Drees F, Pokutta S, Yamada S, Nelson W and Weis W. Alpha-catenin is a molecular switch that binds E-cadherin-beta-catenin and regulates actin-filament assembly. Cell 2005; 123: 903-15.

[11] Yang J, Mani S, Donaher J, Ramaswamy S, Itzykson R, Come C, Savagner P, Gitelman I, Richardson A and Weinberg R. Twist, a master regulator of morphogenesis, plays an essential role in tumor metastasis. Cell 2004; 117: 927-39.

[12] Maretzky T, Reiss K, Ludwig A, Buchholz J, Scholz F, Proksch E, de Strooper B, Hartmann D and Saftig P. ADAM10 mediates E-cadherin shedding and regulates epithelial cell-cell ad-

hesion, migration, and beta-catenin translocation. Proc Natl Acad Sci U S A 2005; 102: 9182-7.
[13] Reiss K, Maretzky T, Ludwig A, Tousseyn T, de Strooper B, Hartmann D and Saftig P. ADAM10 cleavage of N-cadherin and regulation of cell-cell adhesion and beta-catenin nuclear signalling. EMBO J 2005; 24: 742-52.
[14] Kim H, Oh M, Lu Q and Kim K. E-cadherin negatively modulates delta-catenin-induced morphological changes and RhoA activity reduction by competing with p190RhoGEF for delta-catenin. Biochem Biophys Res Commun 2008; 377: 636-41.
[15] Kim H, He Y, Yang I, Zeng Y, Kim Y, Seo Y, Murnane M, Jung C, Lee J, Min J, Kwon D, Kim K, Lu Q and Kim K. δ-catenin promotes E-cadherin processing and activates β-catenin-mediated signaling: implications on human prostate cancer progression. Biochim Biophys Acta 2012; 1822: 509-21.
[16] Nugent M and Iozzo R. Fibroblast growth factor-2. Int J Biochem Cell Biol 2000; 32: 115-20.
[17] Faham S, Hileman R, Fromm J, Linhardt R and Rees D. Heparin structure and interactions with basic fibroblast growth factor. Science 1996; 271: 1116-20.
[18] Fessler E, Borovski T and Medema J. Endothelial cells induce cancer stem cell features in differentiated glioblastoma cells via bFGF. Mol Cancer 2015; 14: 157.
[19] Kigel B, Rabinowicz N, Varshavsky A, Kessler O and Neufeld G. Plexin-A4 promotes tumor progression and tumor angiogenesis by enhancement of VEGF and bFGF signaling. Blood 2011; 118: 4285-96.
[20] Helley D, Banu E, Bouziane A, Banu A, Scotte F, Fischer A and Oudard S. Platelet microparticles: a potential predictive factor of survival in hormone-refractory prostate cancer patients treated with docetaxel-based chemotherapy. Eur Urol 2009; 56: 479-84.
[21] He Y, Ryu T, Shrestha N, Yuan T, Kim H, Shrestha H, Cho Y, Seo Y, Song W and Kim K. Interaction of EGFR to δ-catenin leads to δ-catenin phosphorylation and enhances EGFR signaling. Sci Rep 2016; 6: 21207.
[22] Kim K, Sirota A, Chen Yh YH, Jones SB, Dudek R, Lanford GW, Thakore C and Lu Q. Dendrite-like process formation and cytoskeletal remodeling regulated by delta-catenin expression. Exp Cell Res 2002; 275: 171-84.
[23] Li M, Nopparat J, Aguilar B, Chen Y, Zhang J, Du J, Ai X, Luo Y, Jiang Y, Boykin C and Lu Q. Intratumor δ-catenin heterogeneity driven by genomic rearrangement dictates growth factor dependent prostate cancer progression. Oncogene 2020; 39: 4358-74.
[24] Kim H, Ki H, Park H and Kim K. Presenilin-1 D257A and D385A mutants fail to cleave Notch in their endoproteolyzed forms, but only presenilin-1 D385A mutant can restore its gamma-secretase activity with the compensatory overexpression of normal C-terminal fragment. J Biol Chem 2005; 280: 22462-72.
[25] He Y, Kim H, Ryu T, Lee K, Choi W, Kim K, Zheng M, Joh Y, Lee J, Kwon D, Lu Q and Kim K. C-Src-mediated phosphorylation of δ-catenin increases its protein stability and the ability of inducing nuclear distribution of β-catenin. Biochim Biophys Acta 2014; 1843: 758-68.
[26] Jain S, Gupta R and Sen R. Rho-dependent transcription termination in bacteria recycles RNA polymerases stalled at DNA lesions. Nat Commun 2019; 10: 1207.
[27] Zhou R, Yang Y, Park S, Nguyen T, Seo Y, Lee K, Lee J, Kim K, Hur J and Kim H. The lichen secondary metabolite atranorin suppresses lung cancer cell motility and tumorigenesis. Sci Rep 2017; 7: 8136.
[28] Hoadley KA, Yau C, Hinoue T, Wolf DM, Lazar AJ, Drill E, Shen R, Taylor AM, Cherniack AD, Thorsson V, Akbani R, Bowlby R, Wong CK, Wiznerowicz M, Sanchez-Vega F, Robertson AG, Schneider BG, Lawrence MS, Noushmehr H, Malta TM; Cancer Genome Atlas Network, Stuart JM, Benz CC and Laird PW. Cell-of-origin patterns dominate the molecular classification of 10,000 tumors from 33 types of cancer. Cell 2018; 173: 291-304, e6.
[29] Gao J, Aksoy BA, Dogrusoz U, Dresdner G, Gross B, Sumer SO, Sun Y, Jacobsen A, Sinha R, Larsson E, Cerami E, Sander C and Schultz N. Integrative analysis of complex cancer genomics and clinical profiles using the cBioPortal. Sci Signal 2013; 6: pl1.
[30] Cerami E, Gao J, Dogrusoz U, Gross B, Sumer S, Aksoy B, Jacobsen A, Byrne C, Heuer M, Larsson E, Antipin Y, Reva B, Goldberg A, Sander C and Schultz N. The cBio cancer genomics portal: an open platform for exploring multidimensional cancer genomics data. Cancer Discov 2012; 2: 401-4.
[31] Hänzelmann S, Castelo R and Guinney J. GSVA: gene set variation analysis for microarray and RNA-seq data. BMC Bioinformatics 2013; 14: 7.
[32] Schaefer C, Anthony K, Krupa S, Buchoff J, Day M, Hannay T and Buetow K. PID: the pathway interaction database. Nucleic Acids Res 2009; 37: D674-9.
[33] Kwabi-Addo B, Ozen M and Ittmann M. The role of fibroblast growth factors and their receptors in prostate cancer. Endocr Relat Cancer 2004; 11: 709-24.
[34] Acevedo L, Barillas S, Weis S, Göthert J and Cheresh D. Semaphorin 3A suppresses VEGF-

mediated angiogenesis yet acts as a vascular permeability factor. Blood 2008; 111: 2674-80.
[35] Oh M, Kim H, Yang I, Park JH, Cong WT, Baek MC, Bareiss S, Ki H, Lu Q and No J. GSK-3 phosphorylates δ-catenin and negatively regulates its stability via ubiquitination/proteosome-mediated proteolysis. J Biol Chem 2009; 284: 28579-89.
[36] Aoki K and Taketo MM. Adenomatous polyposis coli (APC): a multi-functional tumor suppressor gene. J Cell Sci 2007; 120: 3327-35.
[37] Chesire D and Isaacs W. Beta-catenin signaling in prostate cancer: an early perspective. Endocr Relat Cancer 2003; 10: 537-60.
[38] Paffenholz R and Franke WW. Identification and localization of a neurally expressed member of the plakoglobin/armadillo multigene family. Differentiation 1997; 61: 293-304.
[39] Ho C, Zhou J, Medina M, Goto T, Jacobson M, Bhide PG and Kosik KS. Delta-catenin is a nervous system-specific adherens junction protein which undergoes dynamic relocalization during development. J Comp Neurol 2000; 420: 261-76.
[40] Peifer M, Berg S and Reynolds AB. A repeating amino acid motif shared by proteins with diverse cellular roles. Cell 1994; 76: 789-91.
[41] Shimizu T, Ishida J, Kurozumi K, Ichikawa T, Otani Y, Oka T, Tomita Y, Hattori Y, Uneda A and Matsumoto Y. δ-catenin promotes bevacizumab-induced glioma invasion. Mol Cancer Ther 2019; 18: 812-22.
[42] Zagzag D, Miller DC, Sato Y, Rifkin DB and Burstein DE. Immunohistochemical localization of basic fibroblast growth factor in astrocytomas. Cancer Res 1990; 50: 7393-98.
[43] Masiero M, Simões FC, Han HD, Snell C, Peterkin T, Bridges E, Mangala LS, Wu SY, Pradeep S, Li D, Han C, Dalton H, Lopez-Berestein G, Tuynman JB, Mortensen N, Li JL, Patient R, Sood AK, Banham AH, Harris AL and Buffa FM. A core human primary tumor angiogenesis signature identifies the endothelial orphan receptor ELTD1 as a key regulator of angiogenesis. Cancer Cell 2013; 24: 229-41.
[44] Brem S, Tsanaclis AM, Gately S, Gross JL and Herblin WF. Immunolocalization of basic fibroblast growth factor to the micro vasculature of human brain tumors. Cancer 1992; 70: 2673-80.
[45] Sieber CC, Sumanovski LT, Stumm M, van der Kooij M and Battegay E. In vivo angiogenesis in normal and portal hypertensive rats: role of basic fibroblast growth factor and nitric oxide. J Hepatol 2001; 34: 644-50.
[46] Nakamoto T, Chang C, Li A and Chodak GW. Basic fibroblast growth factor in human prostate cancer cells. Cancer Res 1992; 52: 571-77.
[47] Rodeck U and Herlyn M. Growth factors in melanoma. Cancer Metastasis Rev 1991; 10: 89-101.
[48] Morrison RS, Giordano S, Yamaguchi F, Hendrickson S, Berger M and Palczewski K. Basic fibroblast growth factor expression is required for clonogenic growth of human glioma cells. J Neurosci Res 1993; 34: 502-9.
[49] Wesley UV, McGroarty M and Homoyouni A. Dipeptidyl peptidase inhibits malignant phenotype of prostate cancer cells by blocking basic fibroblast growth factor signaling pathway. Cancer Res 2005; 65: 1325-34.
[50] Nguyen M, Watanabe H, Budson AE, Richie JP, Hayes DF and Folkman J. Elevated levels of an angiogenic peptide, basic fibroblast growth factor, in the urine of patients with a wide spectrum of cancers. J Natl Cancer Inst 1994; 86: 356-61.
[51] Tanaka K, Abe M and Sato Y. Roles of extracellular signal-regulated kinase 1/2 and p38 mitogen-activated protein kinase in the signal transduction of basic fibroblast growth factor in endothelial cells during angiogenesis. Jpn J Cancer Res 1999; 90: 647-54.
[52] Im HJ, Muddasani P, Natarajan V, Schmid TM, Block JA, Davis F, van Wijnen AJ and Loeser RF. Basic fibroblast growth factor stimulates matrix metalloproteinase-13 via the molecular cross-talk between the mitogen-activated protein kinases and protein kinase Cδ pathways in human adult articular chondrocytes. J Biol Chem 2007; 282: 11110-21.
[53] Walsh CT, Wei Y, Wientjes MG and Au JL. Quantitative image analysis of intra-tumoral bFGF level as a molecular marker of paclitaxel resistance. J Transl Med 2008; 6: 1-10.
[54] Hong BZ, Park SA, Kim HN, Ma TZ, Kim HG, Kang HS, Kim HG and Kwak YG. Basic fibroblast growth factor increases intracellular magnesium concentration through the specific signaling pathways. Mol Cells 2009; 28: 13-17.
[55] Song G, Ouyang G and Bao S. The activation of Akt/PKB signaling pathway and cell survival. J Cell Mol Med 2005; 9: 59-71.
[56] Raman M, Chen W and Cobb M. Differential regulation and properties of MAPKs. Oncogene 2007; 26: 3100-12.
[57] Kim K, Oh M, Ki H, Wang T, Bareiss S, Fini M, Li D and Lu Q. Identification of E2F1 as a positive transcriptional regulator for delta-catenin. Biochem Biophys Res Commun 2008; 369: 414-20.

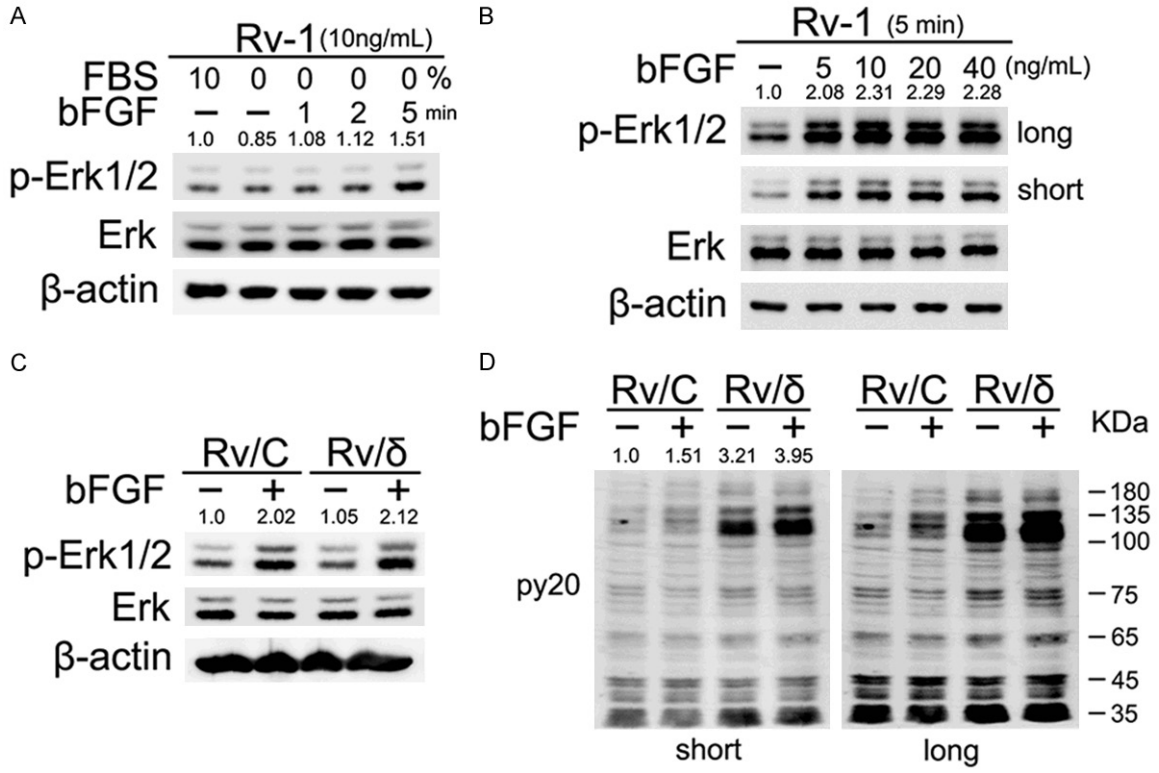

Supplementary Figure 1. The action of bFGF is dose- and time-dependent in Rv-1 cells. A. Before starting the experimental procedures, the medium was removed and replaced with serum-free medium for 30 min (only this time). Rv-1 cells were cultured in serum-free medium in the presence or absence of bFGF (10 ng/ml) for 1, 2, and 5 min. B. Rv-1 cells were cultured in serum-free medium (2 h) in the presence or absence of bFGF (5, 10, 20, and 40 ng/ml) for 5 min. C, D. Both Rv/δ and Rv/C cells were cultured in serum-free medium (2 h) in the presence or absence of bFGF (20 ng/ml) for 5 min and subjected to immunoblotting.

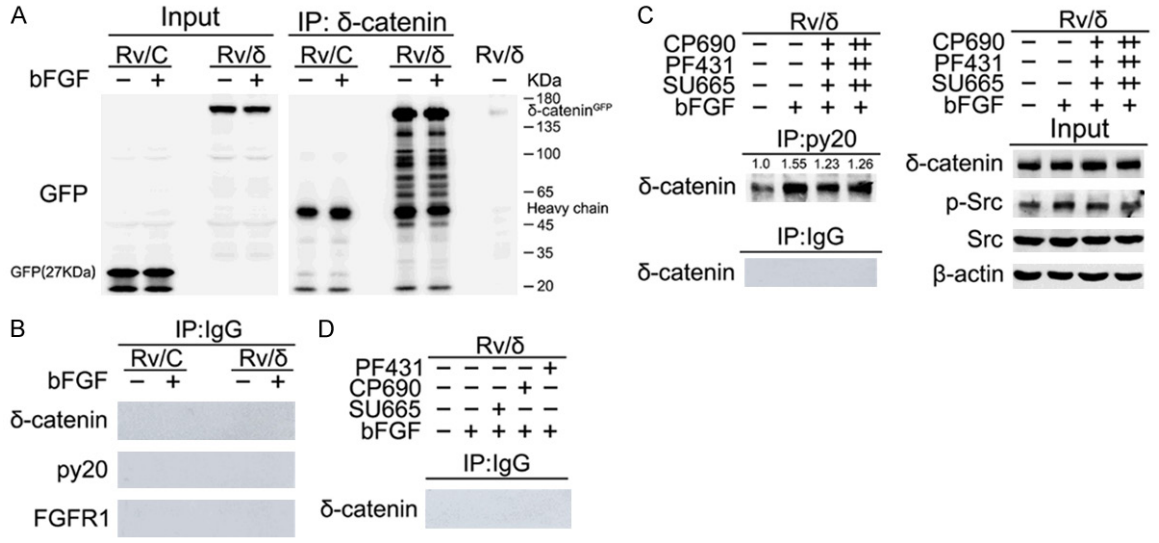

Supplementary Figure 2. δ-catenin is phosphorylated by bFGF in an FGFR1-dependent but tyrosine kinase-independent manner. A, B. Both Rv/C and Rv/δ cells were cultured in serum-free medium (2 h) in the presence or absence of bFGF (20 ng/ml) for 5 min. A. The cell lysates were subjected to immunoprecipitation with δ-catenin antibody followed by immunoblotting with GFP antibody. B. Cell lysates were also subjected to immunoprecipitation with IgG as negative control. C. Rv/δ cells were co-treated with Src (SU665, 100 nM), FAK (PF431396, 500 nM),

and JAK (CP690550, 500 nM) kinase inhibitors for 2 h in serum-free medium before harvesting. The cell lysates were used to perform immunoblotting to analyze the protein expression of p-Src, Src, and β-actin and were also subjected to immunoprecipitation with the py20 antibody followed by immunoblotting with the δ-catenin antibody. Cell lysates were also subjected to immunoprecipitation with IgG as negative control. D. Rv/δ cells were respectively pretreated with Src (SU665, 100 nM), FAK (PF431396, 500 nM), and JAK (CP690550, 500 nM) kinase inhibitors for 2 h in serum-free medium before harvesting. Cell lysates were subjected to immunoprecipitation with IgG as negative control.

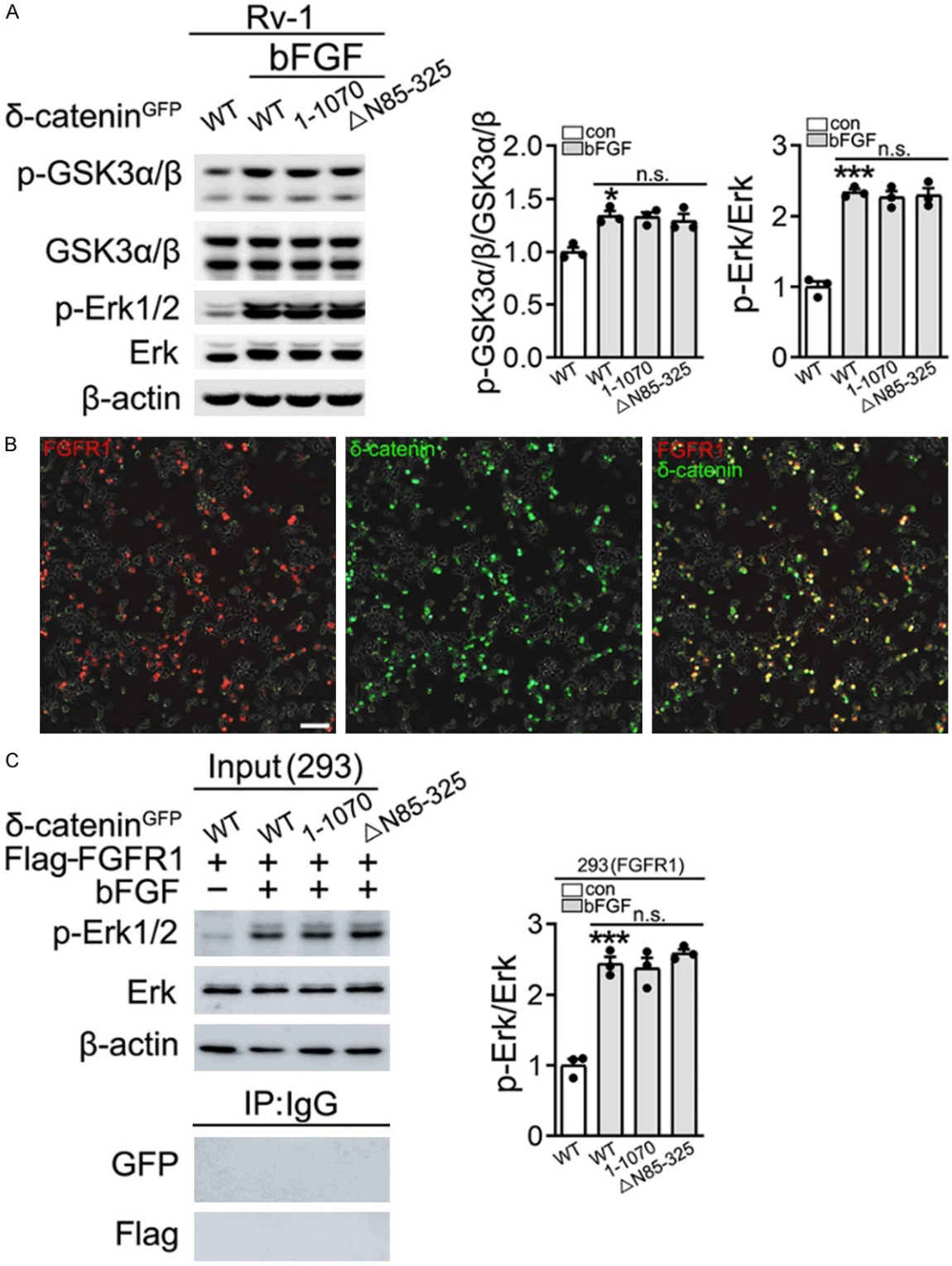

Supplementary Figure 3. The downstream bFGF/FGFR1 signaling pathway did not change compare with different groups after bFGF treatment. A. Rv-1 cells were transfected with the constructs of GFP-δ-catenin WT and its different deletions in the presence or absence of bFGF. The cell lysates were subjected to immunoblotting with the relative antibody to analyze protein expression. Quantitative analysis is shown as a bar graph in the right panel. The values are presented as the mean ± SEM of three independent experiments. $^{*}P < 0.05$ vs. control; $^{***}P < 0.01$ vs. control; n.s. = not significant. B. Transfection of mCherry-FGFR1 and GFP-δ-catenin WT or its different deletions was performed in 293 cells. The cells were observed with a computer-assisted microscope (EVOS, Thermo Fisher Scientific, MA, United States). Scale bar = 110 μm. Red: FGFR1, Green: δ-catenin. C. The 293 cells were treatment with the presence or absence of bFGF and the cell lysates were subjected to immunoblotting to check protein expression. Quantitative analysis is shown as a bar graph in the right panel. Cell lysates were also subjected to immunoprecipitation with IgG as negative control. The values are presented as the mean ± SEM of three independent experiments. $^{***}P < 0.01$ vs. control; n.s. = not significant.

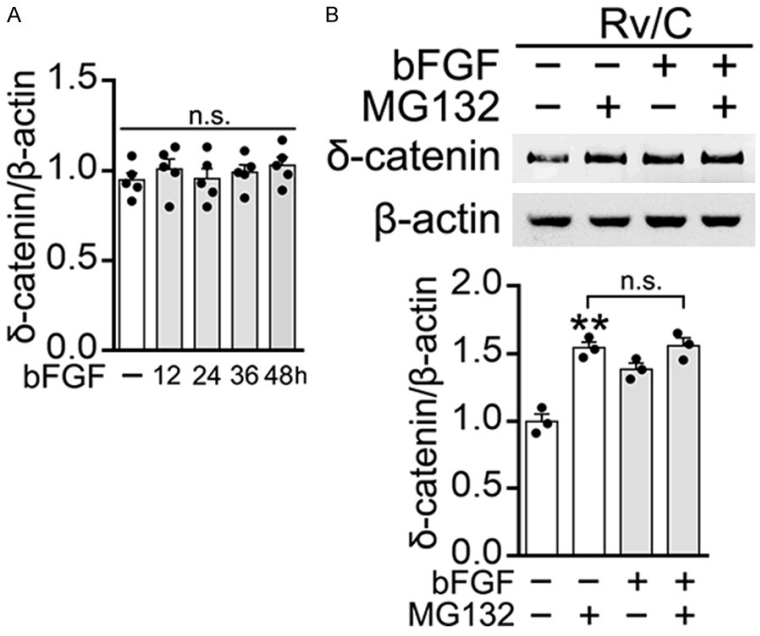

Supplementary Figure 4. bFGF treatment does not affect δ-catenin mRNA levels in Rv-1 cells. A. The mRNA expression of the δ-catenin gene in Rv-1 cells. The values displayed are the mean ± SEM of five independent experiments. The two-tailed Student's t-test was used, n.s. = not significant. B. Rv/C cells were treated with or without bFGF (20 ng/ml) and MG132 (20 μg/ml) for 12 h. The cell lysates were subjected to immunoblotting with the δ-catenin antibody to analyze protein expression. Quantitative analysis is shown as a bar graph in the lower panel. The values are presented as the mean ± SEM of three independent experiments. $^{**}P < 0.01$ vs. control; n.s. = not significant.

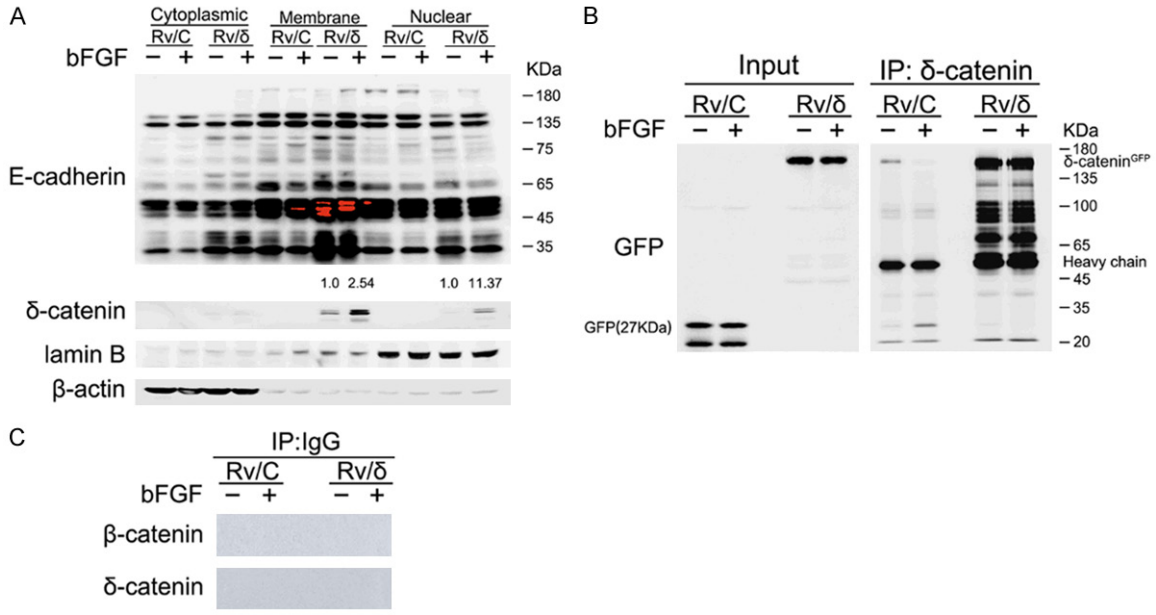

Supplementary Figure 5. bFGF increases δ-catenin ability to enhance the nuclear distribution of β-catenin by disturbing the integrity of the E-cadherin. Both Rv/δ and Rv/C cells were treated with or without bFGF (20 ng/ml) for 12 h. A. Both Rv/δ and Rv/C cells were subjected to the fractionation experiment. B. The cell lysates were subjected to immunoprecipitation with the δ-catenin antibody followed by immunoblotting with the GFP antibody. C. Cell lysates were also subjected to immunoprecipitation with IgG as negative control.

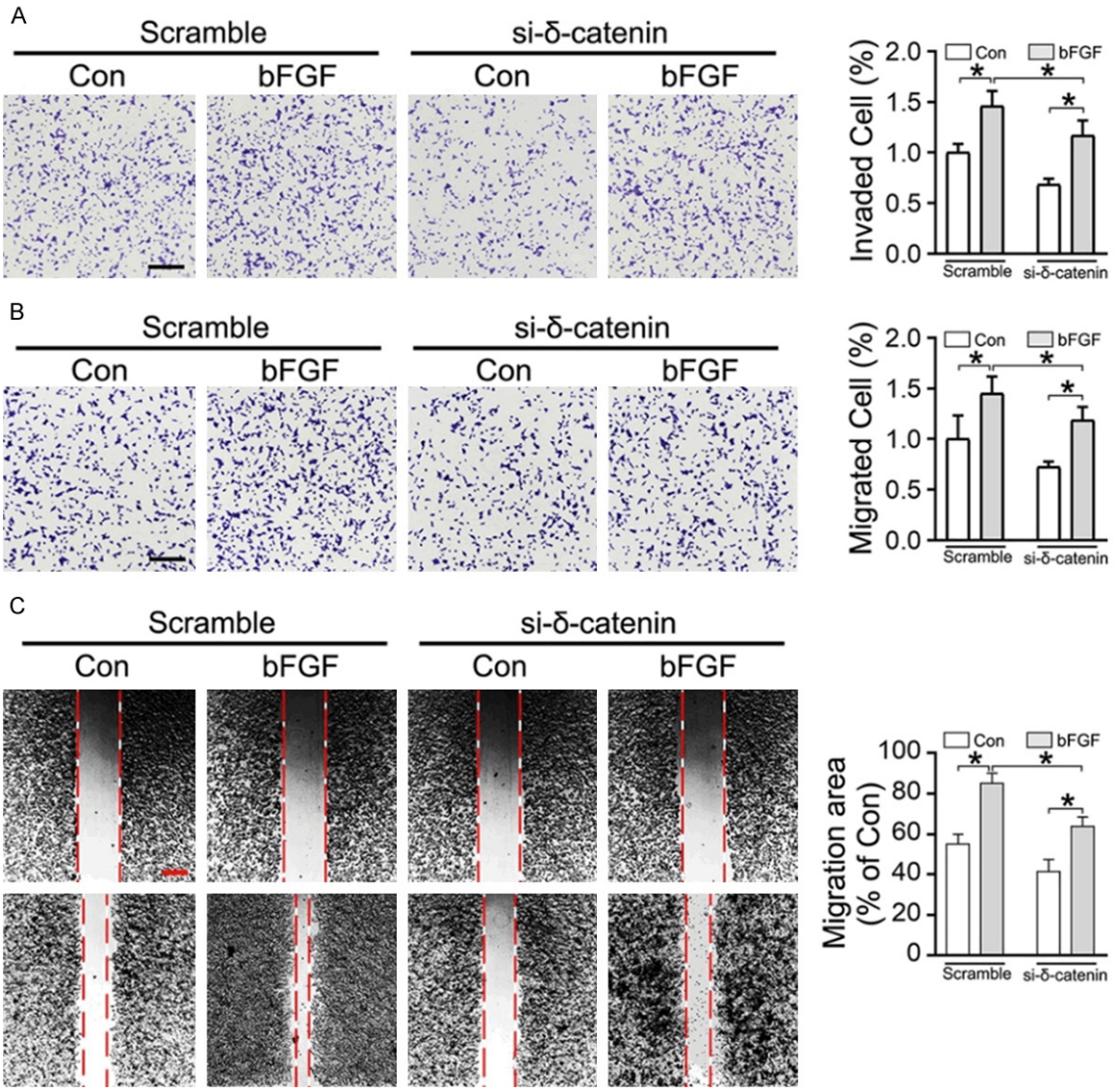

Supplementary Figure 6. bFGF increase the motility of prostate cancer cells via δ-catenin. δ-catenin siRNA was used to transfected cells with LipofectamineTM 2000 reagent (Invitrogen) for 24 h and cells were treated in the presence or absence of bFGF (20 ng/ml). (A, B) Invasion and migration assays were performed in the presence or absence of bFGF. Transwell chambers coated with (A) or without (B) gelatin, respectively. Quantitative analysis of cell viability, colony area, and migrated and invaded cell numbers from at least three independent experiments are shown as a bar graph in each right panel. Scale bar = 260 μm. The values are presented as the mean ± SEM. $^{*}P < 0.05$. (C) Representative migration across a scratch (magnification at t = 0 and 36 h; dotted lines indicate boundary of the scratch) and area under the curve from Rv-1 cells cultured in the indicated media. Scale bar = 130 μm. Cell migration distances were measured based on the data, with each data point representing the mean of multiple measures within a single well in a representative experiment, values displayed are means ± SEM of three independent experiments. One-way ANOVA with the Student-Newman-Keuls test was used. $^{*}P < 0.05$.